JACS
JOURNAL OF THE AMERICAN CHEMICAL SOCIETY

pubs.acs.org/JACS

Article

Dynamic Assemblies of Molecular Motor Amphiphiles Control Macroscopic Foam Properties

Shaoyu Chen, Franco King-Chi Leung,* Marc C. A. Stuart, Chaoxia Wang,* and Ben L. Feringa*

Cite This: *J. Am. Chem. Soc.* 2020, 142, 10163−10172

Read Online

ACCESS | Metrics & More | Article Recommendations | Supporting Information

ABSTRACT: Stimuli-responsive supramolecular assemblies controlling macroscopic transformations with high structural fluidity, i.e., foam properties, have attractive prospects for applications in soft materials ranging from biomedical systems to industrial processes, e.g., textile coloring. However, identifying the key processes for the amplification of molecular motion to a macroscopic level response is of fundamental importance for exerting the full potential of macroscopic structural transformations by external stimuli. Herein, we demonstrate the control of dynamic supramolecular assemblies in aqueous media and as a consequence their macroscopic foam properties, e.g., foamability and foam stability, by large geometrical transformations of dual light/heat stimuli-responsive molecular motor amphiphiles. Detailed insight into the reversible photoisomerization and thermal helix inversion at the molecular level, supramolecular assembly transformations at the microscopic level, and the stimuli-responsive foam properties at the macroscopic level, as determined by UV−vis absorption and NMR spectroscopies, electron microscopy, and foamability and *in situ* surface tension measurements, is presented. By selective use of external stimuli, e.g., light or heat, multiple states and properties of macroscopic foams can be controlled with very dilute aqueous solutions of the motor amphiphiles (0.2 weight%), demonstrating the potential of multiple stimuli-responsive supramolecular systems based on an identical molecular amphiphile and providing opportunities for future soft materials.

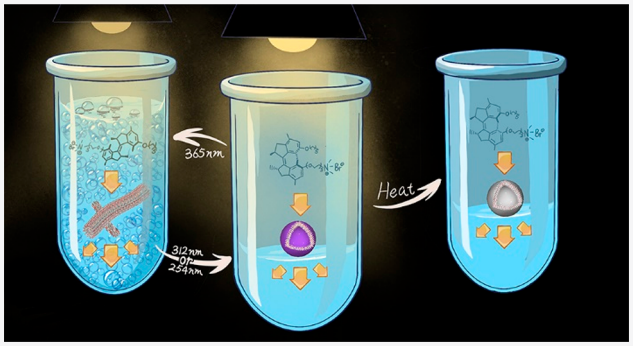

INTRODUCTION

Controlled supramolecular assembly of biomolecules into functional structures with low structural fluidity, e.g., cytoskeleton filaments,[1,2] flagellar filaments of bacteria,[3,4] and high structural fluidity, e.g., cell membranes,[5,6] serve key roles in correct functioning of biological processes. Inspired by natural supramolecular polymers,[1−4] the delicate structural tunability and stimuli-responsiveness of synthetic supramolecular polymers[7−16] in aqueous media allow sophisticated bioinspired functionality.[8−19] A molecular design with precise control of molecular organization and cooperativity enables energy conversion and amplification from nanometer to macroscopic length scales and induces a mechanical response[20−30] in hierarchical supramolecular assemblies.[31−38] Stimuli-responsive amphiphilic molecules can assemble from one-dimensional (1D) systems with low structural fluidity at microscopic length scales to various three-dimensional (3D) macroscopic supramolecular structures, to gain full control of macroscopic structural transformations by the cooperative action of molecular motion.[39−41] For instance, using external stimuli, e.g., pH,[38] heat,[42] and light,[43−48] the isomerization of stimuli-responsive molecules can induce a macroscopic rupture of the 3D randomly entangled supramolecular structures from a gel state into a solution state. In addition to gel−sol transformations, we recently reported that a photoresponsive hierarchical supramolecular macroscopic string of a motor amphiphile allows the amplification of molecular rotation to macroscopic muscle-like contraction.[31−33] However, macroscopic structural transformations and collective behavior usually require a high concentration of stimuli-responsive units as well as high structurally ordered and rigid supramolecular assemblies.[31−33,38,42] Alternatively, as inspired by nature, e.g., the cell membrane, a supramolecular assembly with high structural fluidity can potentially be constructed with a minimized amount of stimuli-responsive units that might allow a more effective energy conversion and amplification from nanometer length-scale motion to macroscopic structural transformations. Foams are a particularly attractive class of soft materials with applications ranging from biomedical systems to industrial processes. Particularly important for textile coloring, photoresponsive foams are highly warranted. By purging aqueous solutions of an amphiphilic molecular structure (in

Received: March 22, 2020
Published: May 7, 2020

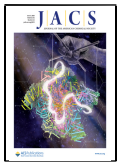

https://dx.doi.org/10.1021/jacs.0c03153
J. Am. Chem. Soc. 2020, 142, 10163−10172

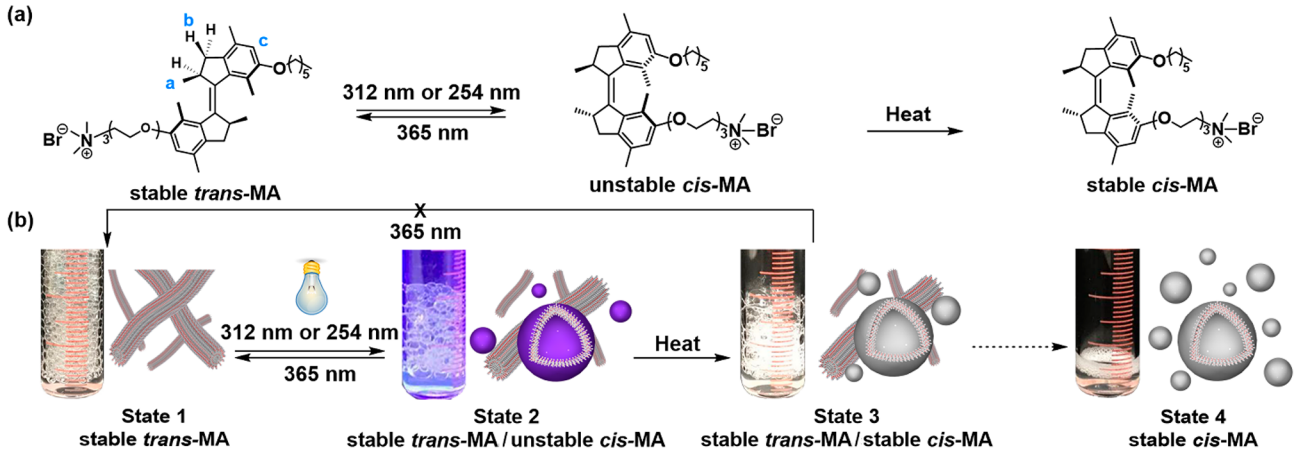

Figure 1. Schematic illustration of (a) the reversible photoisomerization and thermal helix inversion of molecular motor amphiphile (**MA**) and (b) the change in macroscopic foaming processes due to structural transformations in the supramolecular assembly. The state 4 is obtained by using synthetically purified stable *cis*-**MA**.

general below 1.0 weight%) with air, macroscopic foams with high structural fluidity are generated by dispersing air bubbles in the aqueous phase.[49−51] The foam structure spans over multilength scales from nanometer dimensions to macroscopic levels.[51] To provide control of macroscopic foam properties, e.g., foamability and foam stability, advantage can be taken of the molecular isomerization of stimuli-responsive amphiphilic structures at molecular length scales.[52−63]

Recently, we and others have demonstrated photoresponsive foams of azobenzene amphiphiles[55−63] for controlling foam rupture upon irradiation. In an alternative approach, a coassembled lipid system showed photo- and thermal-responsive transformation based on heat produced upon irradiation.[64,65] The noninvasive and reversible control of molecular interactions and function in water over length scales from molecular motions to assembly transformations at the microscopic level and precise control of multiple-state foam properties at the macroscopic level remains challenging. The amphiphiles used to date typically have two states triggered by light, limiting the development of more subtle and precisely controllable foams with multiple states which is crucial for practical applications. Also, the coupling of several reversible isomerization processes in a single photoresponsive molecular system to dynamic assembly formation at the microscopic scale in order to identify the key processes for energy conversion from nanometer-length-scale motion to macroscopic structural transformations, i.e., macroscopic foam rupture, remains largely unexplored. We envisioned that the development of a robust stimuli-responsive amphiphile with multiple states and intrinsic foam properties would not only allow more sophisticated control over foamability but also reveal how to achieve dynamic regulation of assemblies in water and enable amplification along length scales.

Here we present a robust molecular motor-based light-responsive amphiphile that has the intrinsic propensity to trigger the formation of multiple states and assemblies in water and allows changes at the nanoscale to be translated to macroscopic properties, i.e., foam formation. To the best of our knowledge, this is also the first amphiphile where we have absolute and unprecedented control over the aggregation behavior, i.e., switching from worm-like structures to vesicles and back without helper lipids or effectuators to get out of a situation where the amphiphile is locked in an (kinetically stable) aggregate.

Molecular motors can be controlled with high precision by two external stimuli, light and heat, to sustain a unidirectional rotation involving four distinct isomerization states. We envision that molecular motor amphiphiles hold significant prospects for the development of multiple states macroscopic foams with a minimized amount of stimuli-responsive units as well as the study of essential parameters for amplification from nanometer-length-scale motion to macroscopic foam properties. We previously reported that motor amphiphiles composed of a second generation molecular motor core used as dopants into lipids provided supramolecular assembly transformations, but extra freeze−thaw cycles were required in the transformation processes.[66−68] Furthermore, the nanofibers of motor amphiphiles employed in artificial muscle-like motions showed no significant supramolecular assembly transformations upon photoirradiation.[31−33] To sustain a large geometrical transformation, the change in packing parameters between *trans*- and *cis*-isomers[69,70] is of fundamental importance for generating supramolecular assembly transformations from an identical molecular structure upon photoisomerization. In the present design, the molecular motor amphiphile contains a hydrophilic chain with a charged end group and a hydrophobic alkyl chain connected to a first-generation molecular motor core (Figure 1). If the motor unit adopts a *trans* geometry, the two side chains will be remote from each other and we expect a lower packing parameter in the structure (e.g., worm-like micelles, $1/3 < P \leq 1/2$), while the *cis* form will bring the two side chains in close proximity, allowing for a higher packing parameter (e.g., vesicles, $1/2 < P \leq 1$).[69,70] Large geometrical transformations of motor amphiphiles might therefore enable supramolecular transformations, without coassembly with other lipids, for controlling macroscopic foam properties. By elucidating the key transformation processes and parameters governing assembly, this could open up new prospects toward the development of externally controlled stimuli-responsive materials.

RESULTS AND DISCUSSION

Molecular Design and Synthesis. The motor amphiphile (**MA**) was designed with a first-generation molecular motor

https://dx.doi.org/10.1021/jacs.0c03153
J. Am. Chem. Soc. 2020, 142, 10163−10172

core, functionalized with an alkyl chain as the hydrophobic part and a quaternary ammonium moiety connected via a triethylene glycol-linker as the hydrophilic part. The synthesis is summarized in Scheme 1. Phenolic motor **1** and 1,2-bis(2-bromoethoxy)-ethane (**3**) were prepared according to previously reported procedures,[71,72] and the stable *trans* and stable *cis* isomers of motor **1** were isolated by flash column chromatography.[71] Motor **2** was obtained by a Williamson ether formation in the presence of 1-bromohexane, tetrabutylammonium iodide, and K_2CO_3 in acetonitrile. The freshly prepared motor **2** was treated with 1,2-bis(2-bromoethoxy)-ethane (**3**) and Cs_2CO_3 in DMF to afford stable *trans*-**4** and stable *cis*-**4** in 43% and 50% yields, respectively. Subsequent reaction of motor **4** with trimethylamine gave the corresponding stable *trans*-**MA** and stable *cis*-**MA** in 90% yield. The detailed procedures of the synthesis are provided in the Supporting Information. The structures of all new molecules were confirmed by ^{1}H, ^{13}C NMR, and high-resolution ESI-MS (see Supporting Information, Figures S11−S18).

Scheme 1. Synthesis of Stable *trans*-MA and Stable *cis*-MA

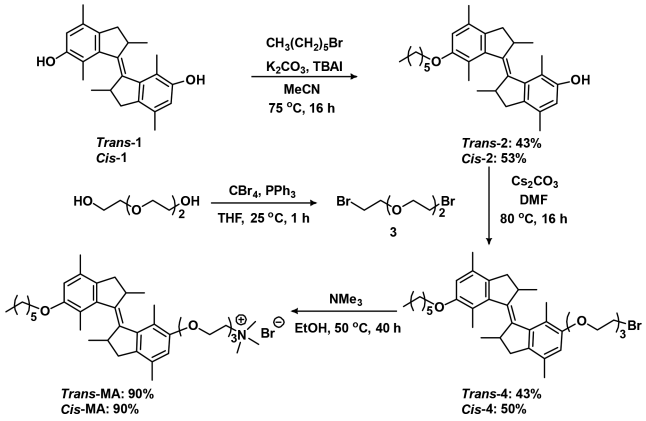

Photoisomerization and Thermal Helix Inversion Steps to Control Packing Parameters of MA. For the first-generation motor core of **MA**, its 360° unidirectional rotary cycle involves four stages, in which one-half of the molecule rotates with respect to the other half around a central double bond via two photochemical isomerization processes and two thermal helix inversion (THI) steps (Figure S2). Because of the fast thermal isomerization between unstable *trans*-**MA** and stable *trans*-**MA** (<10 s at rt),[73,74] only the reversible photoisomerization from stable *trans*-**MA** to unstable *cis*-**MA** as well as the THI between unstable *cis*-**MA** and stable *cis*-**MA** are employed for the three-stage control of the modulation of molecular geometries and, as a consequence, packing parameter transformations (Figure 1). First, the proper functioning of the motor amphiphiles *trans*-**MA** and *cis*-**MA** was studied in an organic solvent (see Figures S3a−c, S4a−c, S5, and Table S1). A methanol solution of stable *trans*-**MA** (30 μM) shows a strong absorption band at 260−340 nm in the UV−vis absorption spectrum (Figure S3a). A new absorption band appears at 340−400 nm with a clear isosbestic point at 330 nm upon 312 nm light irradiation for 6 min at 5 °C (Figure S3a), indicating a selective photoisomerization process from stable *trans*-**MA** to unstable *cis*-**MA**. The resulting solution, prepared by the photoisomerization from stable *trans*-**MA** to unstable *cis*-**MA**, showed the reverse switching process to stable *trans*-**MA** upon 365 nm light irradiation for 1 min (Figure S3b), or the selective rotation from unstable *cis*-**MA** to stable *cis*-**MA** by heating at 55 °C for 2 h via the THI step (Figure S3c). A CD_3OD solution of stable *trans*-**MA** (2.0 mM) shows distinctive proton shifts in the ^{1}H NMR spectra upon isomerization (Figure S4a−c). The proton signals of H_a (δ = 1.10 ppm) and H_b (δ = 2.18 ppm) shift downfield to δ = 1.23 ppm and δ = 2.60 ppm, respectively, while an upfield shift of H_c is observed with an unstable *cis*-**MA**/stable *trans*-**MA** isomer ratio of 1:1, upon 312 nm light irradiation for 6 min (Figure S4a,b). Notably, the obtained unstable *cis*-**MA** in the solution can be fully switched back to stable *trans*-**MA** with 365 nm light irradiation, or selectively isomerized to stable *cis*-**MA** by heating at 55 °C for 2 h via the THI step with a distinct set of proton shifts (H_a: δ = 1.23 ppm to 1.05 ppm, H_b: δ = 2.60 ppm to 2.41 ppm; Figure S4a−c). The rate constants of the thermal isomerization process from unstable *cis*-**MA** to stable *cis*-**MA** were studied by means of Eyring analysis (Figure S5), and a standard Gibbs energy of activation ($\Delta^{\ddagger}G°$ = 100.0 kJ mol^{-1}) was obtained, which corresponds to a half-life of 10.6 h at 25 °C (Table S1). The results clearly demonstrated that the geometrical transformations could be controlled selectively by external stimuli light and heat in methanol.

Next, the motor amphiphiles were studied in aqueous media (Figures S3d−f, S4d−f, S6, 2, and S7). A Tris-EDTA buffer (pH 7.4) solution of stable *trans*-**MA** (30 μM) shows an absorption band at 260−340 nm in the absorption spectrum;

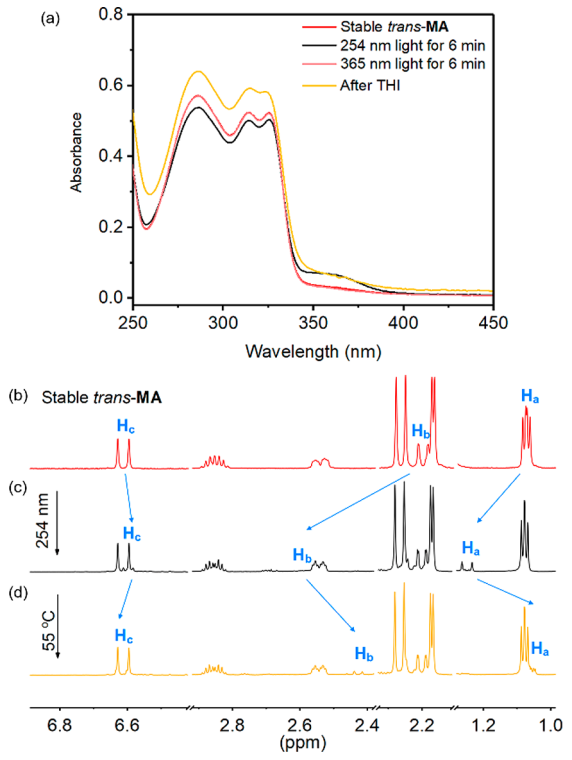

Figure 2. (a) UV−vis absorption spectra during the 180° rotation process of **MA** (30 μM), from stable *trans*-**MA** to stable *cis*-**MA** in aq. buffer solution (Tris-EDTA, pH 7.4). Aromatic and aliphatic region in the ^{1}H NMR spectra during the isomerization process of **MA** (2.0 mM, CD_3OD, 25 °C, 500 MHz). (b) A buffer solution of stable *trans*-**MA** was (c) irradiated with 254 nm light at 25 °C for 6 min, (d) followed by heating at 55 °C for 24 h (see also Figure S4). The buffer solutions after irradiation or THI step were subjected to a freeze-drying process, and the compound was dissolved in CD_3OD for ^{1}H NMR studies. For the proton assignment, see Figure 1.

https://dx.doi.org/10.1021/jacs.0c03153
J. Am. Chem. Soc. 2020, 142, 10163−10172

however, only a weak absorption band is observed at 340−400 nm upon irradiating with 312 nm light for 6 min at 5 °C (Figure S3d). Consequently, an unstable *cis*-**MA**/stable *trans*-**MA** isomer ratio of only 1:22 is obtained in a buffer solution of stable *trans*-**MA** (2.0 mM) irradiated with 312 nm light for 6 min, as shown by the ^{1}H NMR spectra (Figure S4d,e). As expected, only limited ratiometric changes in the absorption spectra and proton signal shifts in the ^{1}H NMR spectra are observed in a buffer solution, containing the mixture of unstable *cis*-**MA**/stable *trans*-**MA** in a 1:22 ratio, upon heating at 55 °C for 2 h (Figures S3f and S4e,f). To allow a more efficient photoisomerization in aqueous media, a higher-energy light source was employed (λ_{max} = 254 nm). A higher unstable *cis*-**MA**/stable *trans*-**MA** isomer ratio of 1:13 was established upon 254 nm light irradiation for 6 min of a buffer solution of stable *trans*-**MA** (2.0 mM) at 5 °C by ^{1}H NMR analysis (Figure S6a). Furthermore, the photoisomerization and THI steps of a buffer solution of stable *trans*-**MA** (30 μM) were followed by UV−vis spectroscopy at 5 °C (Figures 2a and S6b−d). As expected, upon increasing the temperature during irradiation at 254 nm from 5 to 25 °C, a higher unstable *cis*-**MA**/stable *trans*-**MA** isomer ratio of 1:6 is observed based on ^{1}H NMR analysis (Figure 2b,c), which is higher than that observed in a buffer solution of stable *trans*-**MA** upon 312 nm light irradiation at 25 °C for 6 min (unstable *cis*-**MA**/stable *trans*-**MA** isomer ratio of 1:12; Figure S7a).

It should be noted that the ratio of 1:6 was obtained upon irradiation for only 6 min, not reaching the photostationary state, but this was sufficient to induce significant self-assembly transformations and macroscopic foam rupture. Furthermore, similar to isomerization in methanol, the obtained unstable *cis*-**MA** in buffer solution, prepared by the photoisomerization of the stable *trans*-**MA** solution with 254 nm light irradiation for 6 min, was able to switch back to stable *trans*-**MA** by 365 nm light irradiation (Figure S7b), or to convert selectively to stable *cis*-**MA** by heating at 55 °C for 24 h via the THI step (Figure 2c,d). The results indicate that molecular changes can be controlled selectively by external stimuli not only in organic solvents but also in water, allowing for further investigations of molecular geometrical transformations at higher length scales in aqueous media.

Supramolecular Assembly Transformation at Microscopic Length Scales. Freshly prepared Tris-EDTA buffer solutions (pH 7.4) of stable *trans*-**MA** (2.0 mM) were diluted into a range of concentrations from 2.0 × 10^{-5} to 2.0 mM for the determination of the critical aggregation concentration (CAC) by using a Nile Red fluorescence assay (NRFA), which probes the internal hydrophobicity of the assemblies.[32,75,76] A significant decrease in blue shift is observed when the concentration of the stable *trans*-**MA** buffer solution is diluted below 0.1 mM (Figure 3). The CAC of the stable *trans*-**MA** buffer solution was determined as 5 μM (Figure 3). It is noted that the concentrations in the buffer solutions of stable *trans*-**MA** used in UV−vis absorption (30 μM) and ^{1}H NMR spectroscopic studies (2.0 mM) were higher than its CAC. The freshly prepared buffer solution of stable *trans*-**MA** (2.0 mM) was irradiated with 254 nm light for 6 min at 25 °C, whereupon the CAC of the resulting solution of **MA** increased to 12 μM (Figure 3). The results imply that a possible transformation of the supramolecular assembly occurs upon irradiation in the buffer solution of **MA**.

The assemblies of **MA** were imaged using cryogenic transmission electron microscopy (cryo-TEM) to investigate

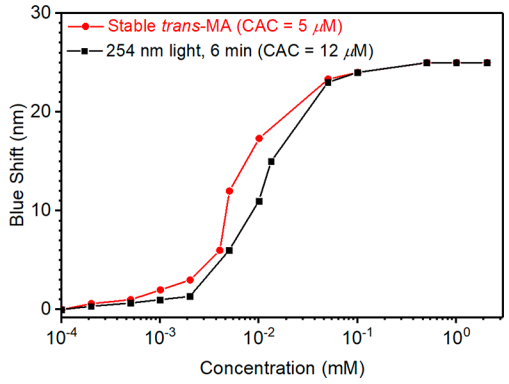

Figure 3. Nile Red fluorescence assay for the determination of the critical aggregation concentration (CAC) of buffer solutions of stable *trans*-**MA** before and after irradiation with 254 nm light for 6 min at 25 °C (concentration: 2.0 × 10^{-5} to 2.0 mM).

their solution-state morphologies. Worm-like micelles with hundreds of nanometers to micrometers in length are observed by the cryo-TEM image of the buffer solution of stable *trans*-**MA** (concentration: 2.0 mM, Figure 4a). A mixture of worm-

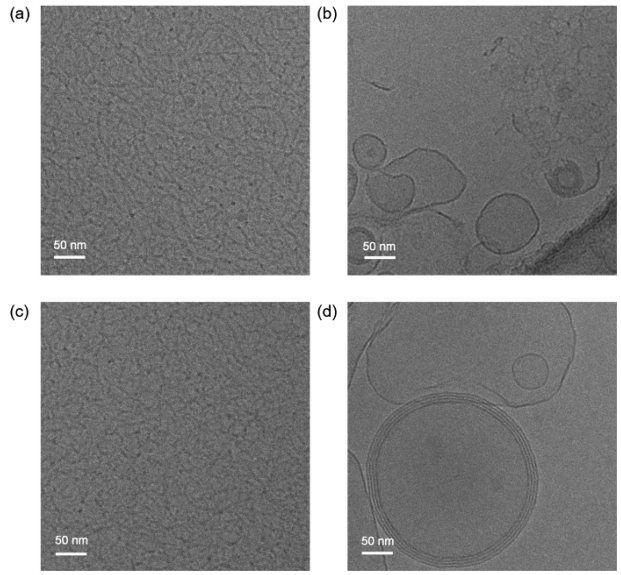

Figure 4. Cryo-TEM images of a buffer solution of stable *trans*-**MA** (2.0 mM) (a) before and (b) after 254 nm light irradiation for 6 min at 25 °C, (c) followed by exposure to 365 nm light for 6 min at 25 °C. (d) A stable *cis*-**MA** buffer solution (2.0 mM).

like micelles/vesicles is observed in the cryo-TEM image of the same solution after 254 nm light irradiation for 6 min at 25 °C (Figure 4b). An identical sample was employed in ^{1}H NMR study (Figure 2c), indicating that the presence of only ∼15% of unstable *cis*-**MA** in the mixture with stable *trans*-**MA** was able to induce a drastic transformation of the supramolecular assembly of **MA** in aqueous media. Notably, the supramolecular assemblies of the mixture of worm-like micelles/vesicles remain stable for 4 h at 25 °C without illumination (Figure S8a−c), but can be reversibly converted back to worm-like micelles after exposure to 365 nm light for 6 min (Figure 4c). An identical sample was used in ^{1}H NMR study (Figure S7b), which demonstrated that the conversion of the mixture of worm-like micelles/vesicles back to worm-like micelles was attributed to the reversible geometrical transformation from

https://dx.doi.org/10.1021/jacs.0c03153
J. Am. Chem. Soc. 2020, 142, 10163−10172

unstable *cis*-**MA** to stable *trans*-**MA**, upon 365 nm light irradiation for 6 min at 25 °C. Furthermore, the buffer solution of stable *trans*-**MA** irradiated with 254 nm light for 6 min and subsequently heated at 55 °C for 24 h shows a mixture of worm-like micelles/vesicles (Figure S8d). Although the obtained morphologies (Figure S8d) are essentially identical to those observed in the sample of stable *trans*-**MA** irradiated with 254 nm light for 6 min at 25 °C (Figure 4b), the obtained vesicle assemblies (Figure S8d) remain stable upon further irradiation with 365 nm light (Figure S8e). Moreover, a freshly prepared buffer solution of stable *cis*-**MA** (2.0 mM) shows vesicle assemblies (Figure 4d), similar to those observed in the sample of stable *trans*-**MA** irradiated with 254 nm light and subsequently heated at 55 °C for 24 h (Figure S8d), suggesting that the obtained mixture of worm-like micelles/vesicles (Figure S8d) is possibly composed of stable *trans*-**MA** and stable *cis*-**MA**. The results showed that the manipulation of molecular geometry with external stimuli can induce the transformations of packing parameters, allowing for the control of supramolecular assemblies from nanometers to hundreds of nanometers length scales systematically. Namely, four states of supramolecular assemblies can be achieved: (1) worm-like micelles from stable *trans*-**MA** only, (2) a mixture of worm-like micelles/vesicles from ~15% of unstable *cis*-**MA** in stable *trans*-**MA** (fully reversible), (3) a mixture of worm-like micelles/vesicles from a mixture of stable *cis*-**MA**/stable *trans*-**MA** which cannot be switched back by 365 nm light irradiation, (4) vesicles from stable *cis*-**MA** only (Figures 1 and 4).

Macroscopic Photoresponsive Foam. Amphiphilic molecules can assemble into supramolecular aggregates in solutions and monolayers at air−water interfaces.[49−51] It is noted that both the supramolecular aggregates and monolayers are highly dependent on the concentration and molecular structure. Therefore, we envisioned that motor amphiphiles in aqueous media and at air−water interfaces might allow the control of macroscopic phenomena by amplification of packing/organization due to geometrical changes. Stable foams were generated from a buffer solution of stable *trans*-**MA** (1.5 mM, 0.4 mL) by bubbling with argon gas (6 cm^3 min^{-1}) for 8 min in a quartz tube (Figure 5a and Movie S1). The buffer solution of stable *trans*-**MA** showed good foamability with a foaming ratio of ~8.3. However, no stable foam was formed by the identical preparation method from a buffer solution of stable *cis*-**MA** (Figure 5a and Movie S1). The foaming ratio (R) was calculated from the equation, $R = V_{foam}/V_{liquid}$, in which V_{foam} and V_{liquid} referred to the foam volume and the original liquid volume to prepare foams, respectively.[63,77] A higher foaming ratio indicates a higher foamability. Drainage[51,78] is one of the main processes resulting in the destabilization of foams, which can be affected by the self-assembled structures in the bulk solutions. Given that long fibrillar assemblies can slow down the drainage process and no significant reduction of drainage process is observed with vesicle assemblies,[64,79,80] the worm-like structures in the solution of stable *trans*-**MA** can prove to be a stable macroscopic foam structure. In sharp contrast, no stable foam was observed in the solution of stable *cis*-**MA**. These promising results provided a hint for the control of macroscopic foam formation and the related foam parameters by using the four states of supramolecular assemblies of **MA** (*vide infra*).

For a buffer solution of stable *trans*-**MA** (2.0 mM) by bubbling with a flow of argon gas (10 cm^3 min^{-1}) for 8 min

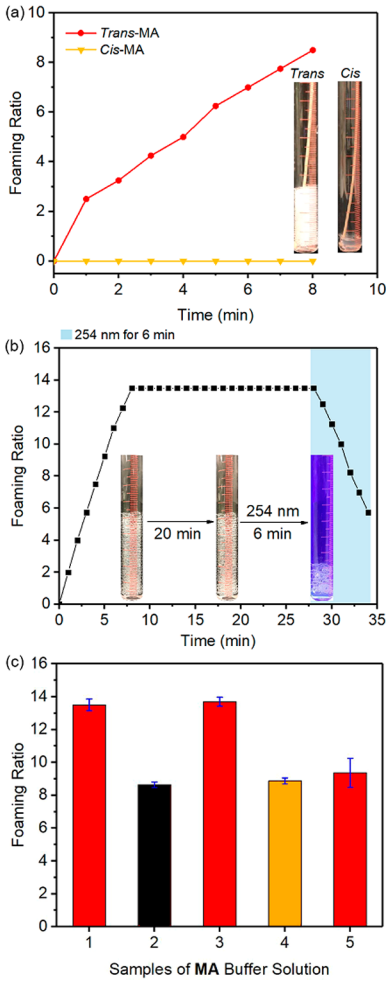

Figure 5. (a) Foamability of stable *trans*-**MA** and stable *cis*-**MA** buffer solutions (1.5 mM, bubbling with a flow of argon gas of 6 cm^3 min^{-1} for 8 min). (b) Foams, prepared from a solution of stable *trans*-**MA** (2.0 mM) by bubbling with a flow of argon gas (10 cm^3 min^{-1} for 8 min), were kept at 25 °C for 20 min and then irradiated with 254 nm light for 6 min. (c) Foamability of stable *trans*-**MA** buffer solutions before and after irradiations and THI steps (2.0 mM, bubbling with a flow of argon gas of 10 cm^3 min^{-1} for 8 min). Stable *trans*-**MA** buffer solutions (sample 1) were irradiated with 254 nm light for 6 min (sample 2). The resulting solutions were exposed to 365 nm light for 6 min (sample 3) or heated at 55 °C for 24 h (sample 4). Sample 4 was subsequently irradiated with 365 nm light for 6 min to obtain sample 5.

(Figure 5b,c, sample 1), a foaming ratio of 13.5 (±0.3) is observed. It is noted that a very diluted stable *trans*-**MA** buffer solution (2.0 mM, containing 99.8 wt % of buffer and 0.2 wt % of **MA**) shows excellent foamability with a high foaming ratio while the foams remain stable over 20 min at 25 °C without any sign of foam rupture (Figure 5b). Notably, fast response of foam rupture, i.e., ~57% of foam rupture, is observed after 254 nm light irradiation at 25 °C for 6 min (Figures 5b). The obtained solutions after foam rupture were subjected to a freeze-drying process and studied by ^{1}H NMR (Figure S9a,b). An unstable *cis*-**MA**/stable *trans*-**MA** isomer ratio of 1:6 is obtained, which is essentially identical to that observed in the buffer solution of stable *trans*-**MA** irradiated with 254 nm light for 6 min at 25 °C (Figure 2b,c). The foam rupture is attributed to the supramolecular assembly transformations from worm-like micelles into the mixture of worm-like

https://dx.doi.org/10.1021/jacs.0c03153
J. Am. Chem. Soc. 2020, 142, 10163−10172

micelles/vesicles as imaged by cryo-TEM (Figure 4a,b). The solution obtained after foam rupture was bubbled with a flow of argon gas (10 cm^3 min^{-1}) for 8 min, which showed a lower foaming ratio of 8.6 ± 0.3 (Figure 5c, sample 2). Furthermore, the resulting solution of stable *trans*-**MA** irradiated with 254 nm light was subsequently exposed to 365 nm light for 6 min at 25 °C, generating stable foams again with a foaming ratio of 13.7 ± 0.3 (Figure 5c, sample 3), comparable to that observed in the solution of stable *trans*-**MA** (2.0 mM; Figure 5b,c; sample 1). Additionally, the obtained solution shows a clear reverse switching process from unstable *cis*-**MA** to stable *trans*-**MA** based on the ^{1}H NMR spectra (Figure S9b,c). The restoration of foamability after sequential irradiation with 254 nm and then 365 nm light is attributed to the transformation from the state (2) a mixture of worm-like micelles/vesicles into the state (1) worm-like micelles, as seen in the cryo-TEM images (Figure 4b,c). Furthermore, the foams obtained from a solution of stable *trans*-**MA** after irradiation with 254 nm light and subsequent heating at 55 °C for 24 h show a foaming ratio of 8.9 ± 0.2 (Figure 5c, sample 4), which is comparable to that observed in the foams obtained from the solution of stable *trans*-**MA** after irradiation with 254 nm light (8.6 ± 0.3, Figure 5c, sample 2). However, when the 254 nm light irradiated solutions of stable *trans*-**MA** were subjected to a THI process (55 °C for 24 h), the foaming ratio of the resulting solution cannot switch back to the value of ∼13 by exposure to 365 nm light (Figure 5c, sample 5).

The results showed clearly that by alternating molecular geometry with light and heat stimuli, the macroscopic foaming ratio also can be finely controlled at four states, i.e., (1) foaming ratio of ∼13 from stable *trans*-**MA** only, (2) a reversible switching of foaming ratio between ∼8 and ∼13 from the photoisomerization of unstable *cis*-**MA** and stable *trans*-**MA**, (3) foaming ratio of ∼8 from a mixture of stable *cis*-**MA**/stable *trans*-**MA** which cannot be switched back by 365 nm light irradiation, (4) no stable foam from stable *cis*-**MA** only (Figure 5). The four states of foaming ratio manipulation were consistent with the four states of supramolecular assembly transformations (Figure 4), indicating the control of macroscopic foam properties by fine adjustment of supramolecular assemblies with external stimuli of light (254 and 365 nm) and heat.

Buffer solutions of stable *trans*-**MA** at 3.0 mM or 4.0 mM by bubbling with a flow of argon gas (10 cm^3 min^{-1} for 8 min) show a comparable foaming ratio (Figure 6a,b) to the foams prepared from the stable *trans*-**MA** solution at 2.0 mM concentration (Figure 5b). The obtained foams, prepared from the stable *trans*-**MA** solutions (at 3.0 mM or 4.0 mM), remain stable over 20 min at 25 °C, and upon exposure to 254 nm light for 6 min, 31% or 14% of foam rupture is observed, respectively (Figure 6a,b). Moreover, the foaming properties can be reversibly tuned by alternating 254 nm light and 365 nm light irradiation over 10 cycles (Figure 6c).

To provide insight into the molecular packing of **MA** at the air−water interface, an *in situ* surface tension measurement was employed. The surface tension was determined by a drop-shape analysis system, which was based on the fitting of the pendant drop shape of the measured solutions with the Yong−Laplace equation of capillarity.[81−83] The detailed experimental setup and measurement conditions are presented in the Supporting Information (Figure S1). The surface tension of the stable *trans*-**MA** buffer solution (2 mM) remains stable at 33.1 mN/m (Figure 7). A quick increase of surface tension

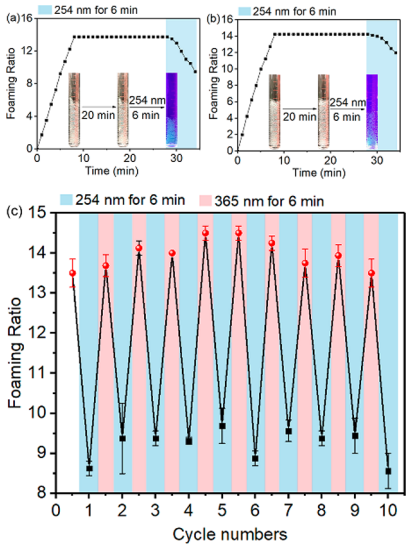

Figure 6. Foams, prepared from solutions of stable *trans*-**MA** at (a) 3.0 mM and (b) 4.0 mM concentration by bubbling with a flow of argon gas (10 cm^3 min^{-1} for 8 min), were kept at 25 °C for 20 min and then irradiated with 254 nm light for 6 min. (c) The change of foaming ratio of a **MA** buffer solution (2.0 mM) after 10 irradiation cycles by alternating 254 and 365 nm light.

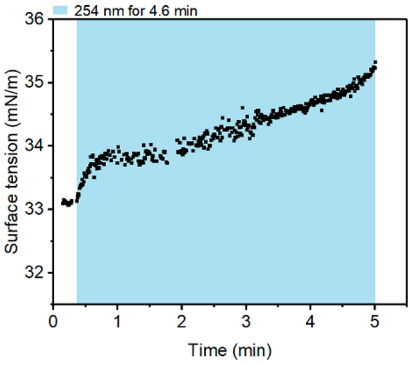

Figure 7. *In situ* surface tension measurement of a droplet of a stable *trans*-**MA** (2.0 mM) buffer solution irradiated with 254 nm light over 4.6 min until the droplet fell down at 5 min.

from 33.1 to 33.9 mN/m was observed after irradiating the droplet of the stable *trans*-**MA** buffer solution with 254 nm light for 30 s. Furthermore, when 254 nm light irradiation was prolonged, the surface tension increased continuously to 35.3 mN/m until the droplet fell down at 5 min; thus the measurement was halted (Figure 7). However, the surface tension of a Tris-EDTA buffer solution irradiated under identical conditions almost remains stable at ∼69.5 mN/m over 5 min (only 0.5 mN/m increase, Figure S10a). The surface tension of a droplet of the stable *trans*-**MA** buffer solution (2 mM) without 254 nm light irradiation also shows limited variation (only 0.5 mN/m increase) over 5 min (Figure S10b). The results clearly indicated that the significant increase of surface tension of the stable *trans*-**MA** buffer solution (up to 2.43 ± 0.27 mN/m) upon irradiation with 254 nm light was attributed to the photoisomerization of stable *trans*-**MA** to unstable *cis*-**MA**.

Following the photochemical isomerization of stable *trans*-**MA** to unstable *cis*-**MA**, a large geometrical transformation is observed, which in turn leads to a disturbance of molecular

https://dx.doi.org/10.1021/jacs.0c03153
J. Am. Chem. Soc. 2020, 142, 10163−10172

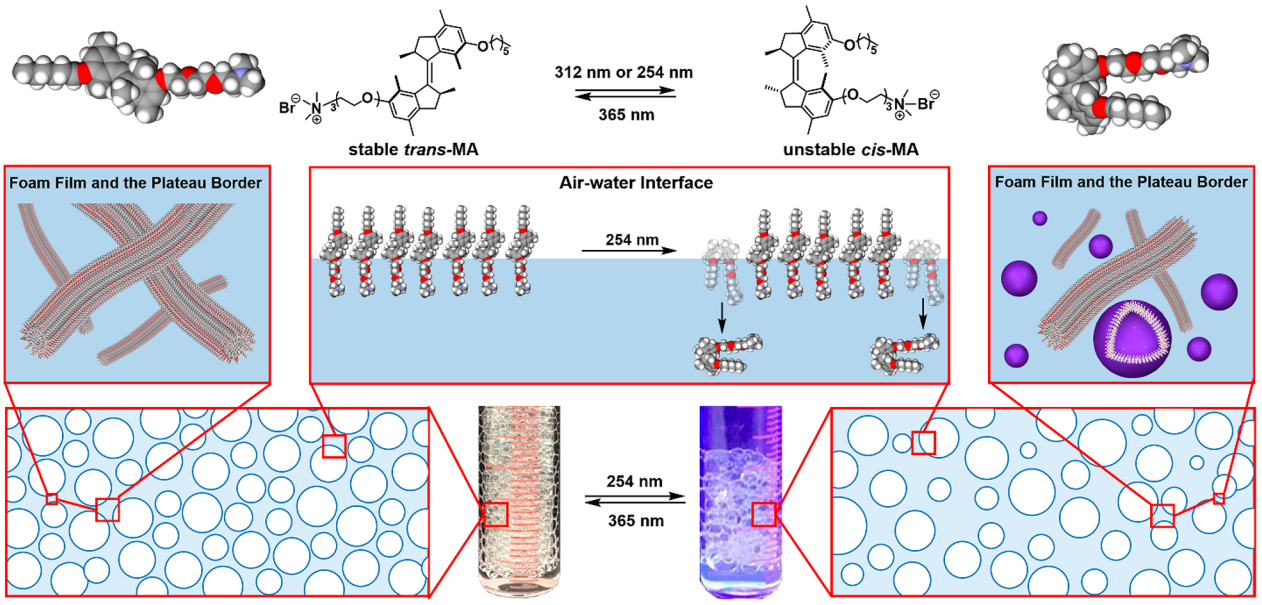

Figure 8. Schematic illustration of supramolecular assembly transformations from stable *trans*-**MA** to unstable *cis*-**MA** upon 254 nm light irradiation at air−water interfaces and in plateau borders.

packing at air−water interfaces.[84] Based on the results of *in situ* surface tension measurements, indeed, a gradual increase of surface tension (up to 2.43 mN/m) was observed, which was attributed to the desorption of unstable *cis*-**MA** from the air−water interfaces to the bulk solution, suggesting that a similar desorption of unstable *cis*-**MA** from the air−water interfaces to the foam films and plateau borders[85] might occur (Figure 8).[81−83] On the basis of supramolecular assembly transformations at the microscopic length scale, long fibrillar structures obtained from the solution of stable *trans*-**MA** result in the reduction of liquid drainage in foams, while a mixture of worm-like micelles/vesicles obtained from the solution of unstable *cis*-**MA**/stable *trans*-**MA** increases the destabilization of foams.[64,79,80] Furthermore, the corresponding transformation from worm-like micelles to the mixture of worm-like micelles/vesicles comes with an increase of CAC (Figure 3), which possibly facilitates the desorption of unstable *cis*-**MA** from the air−water interface to the foam films and the plateau borders. In combination of the aforementioned variation of macroscopic foam parameters, as the ultimate result, foam rupture is observed.

CONCLUSIONS

Amphiphilic motors to control foam properties were designed, and the reversible photoisomerization and thermal helix inversion were followed by UV−vis absorption and proton NMR spectroscopies. As shown by NRFA, a clear increase of CAC of stable *trans*-**MA** was observed after irradiation. By sequential control with light and heat, worm-like micelles of stable *trans*-**MA**, vesicles of stable *cis*-**MA**, and a mixture of worm-like micelles/vesicles of stable *trans*-**MA**/unstable *cis*-**MA** or stable *trans*-**MA**/stable *cis*-**MA** were obtained and analyzed by cryo-TEM. Our responsive system allows a systematic control of macroscopic foam properties and achieves a fine adjustment of foaming ratio over 10 cycles with a low content of **MA** in aqueous media (0.2 wt %). The current approach demonstrates the dual control of multiple state macroscopic foam properties by supramolecular assembly transformations based on light/heat responsive motor amphiphiles. We also identified the key processes and parameters of amplification from molecular motion to macroscopic structural transformations. Besides controlling macroscopic foam properties, it might open up new prospects to generate externally controlled stimuli-responsive soft materials.

ASSOCIATED CONTENT

Supporting Information

The Supporting Information is available free of charge at https://pubs.acs.org/doi/10.1021/jacs.0c03153.

Foamability comparison between stable *trans*-**MA** and stable *cis*-**MA** buffer solution (MP4)

Synthesis, ^{1}H and ^{13}C NMR spectra, UV−vis spectra, cryo-TEM images, surface tension curves (PDF)

AUTHOR INFORMATION

Corresponding Authors

Franco King-Chi Leung − *Center for System Chemistry, Stratingh Institute for Chemistry, University of Groningen, 9747 AG Groningen, The Netherlands;* orcid.org/0000-0003-0895-9307; Email: kingchifranco.leung@polyu.edu.hk

Chaoxia Wang − *Key Laboratory of Eco-Textile, Ministry of Education, College of Textiles Science and Engineering, Jiangnan University, Wuxi 214122, People's Republic of China;* orcid.org/0000-0001-6322-7606; Email: wangchaoxia@sohu.com

Ben L. Feringa − *Center for System Chemistry, Stratingh Institute for Chemistry, University of Groningen, 9747 AG Groningen, The Netherlands;* orcid.org/0000-0003-0588-8435; Email: b.l.feringa@rug.nl

Authors

Shaoyu Chen − *Center for System Chemistry, Stratingh Institute for Chemistry, University of Groningen, 9747 AG Groningen, The Netherlands; Key Laboratory of Eco-Textile, Ministry of Education, College of Textiles Science and Engineering, Jiangnan*

https://dx.doi.org/10.1021/jacs.0c03153
J. Am. Chem. Soc. 2020, 142, 10163−10172

University, Wuxi 214122, People's Republic of China; orcid.org/0000-0003-3029-8568

Marc C. A. Stuart − *Center for System Chemistry, Stratingh Institute for Chemistry, University of Groningen, 9747 AG Groningen, The Netherlands;* orcid.org/0000-0003-0667-6338

Complete contact information is available at: https://pubs.acs.org/10.1021/jacs.0c03153

Notes

The authors declare no competing financial interest.

■ ACKNOWLEDGMENTS

This work was supported financially by the China Scholarship Council (No. 201706790063 to S.Y.C.), the Croucher Foundation (Croucher Postdoctoral Fellowship to F.K.C.L.), The Netherlands Organization for Scientific Research (NWO-CW), the European Research Council (ERC; Advanced Grant No. 694345 to B.L.F.), the Ministry of Education, Culture and Science (Gravitation Program No. 024.001.035) and National Natural Science Foundation of China (21174055), National First-Class Discipline Program of Light Industry Technology and Engineering (LITE2018-21), 111 Project (B17021), the Postgraduate Research & Practice Innovation Program of Jiangsu Provence (No. KYCX17_1435 to S.Y.C.), and the Excellent Doctoral Cultivation Project of Jiangnan University. The authors thanks L. Rohrbach for the technical support in the surface tension measurements.

■ REFERENCES

(1) Fletcher, D. A.; Mullins, R. D. Cell Mechanics and the Cytoskeleton. *Nature* **2010**, *463*, 485−492.
(2) Huber, F.; Schnauß, J.; Rönicke, S.; Rauch, P.; Müller, K.; Fütterer, C.; Käs, J. Emergent Complexity of the Cytoskeleton: From Single Filaments to Tissue. *Adv. Phys.* **2013**, *62*, 1−112.
(3) Lino, T. Assembly of Salmonella Flagellin in Vitro and in Vivo. *J. Supramol. Struct.* **1974**, *2*, 372−384.
(4) Simmons, N. S.; Blout, E. R. The Structure of Tobacco Mosaic Virus and its Components: Ultraviolet Optical Rotatory Dispersion. *Biophys. J.* **1960**, *1*, 55−62.
(5) Chapman, D. Phase Transitions and Fluidity Characteristics of Lipids and Cell Membranes. *Q. Rev. Biophys.* **1975**, *8*, 185−235.
(6) Cooper, R. A. Influence of Increased Membrane Cholesterol on Membrane Fluidity and Cell Function in Human Red Blood Cells. *J. Supramol. Struct.* **1978**, *8*, 413−430.
(7) Lehn, J. M. Supramolecular Polymer Chemistry-Scope and Perspective. *Polym. Int.* **2002**, *51*, 825−839.
(8) Oshovsky, G. V.; Reinhoudt, D. N.; Verboom, W. Supramolecular Chemistry in Water. *Angew. Chem., Int. Ed.* **2007**, *46*, 2366−2393.
(9) de Greef, T. F. A.; Meijer, E. W. Supramolecular Polymers. *Nature* **2008**, *453*, 171−173.
(10) Palmer, L. C.; Stupp, S. I. Molecular Self-Assembly into One-Dimensional Nanostructures. *Acc. Chem. Res.* **2008**, *41*, 1674−1684.
(11) Wojtecki, R. J.; Meador, M. A.; Rowan, S. J. Using the Dynamic Bond to Access Macroscopically Responsive Structurally Dynamic Polymers. *Nat. Mater.* **2011**, *10*, 14−27.
(12) Krieg, E.; Rybtchinski, B. Noncovalent Water-Based Materials: Robust yet Adaptive. *Chem. - Eur. J.* **2011**, *17*, 9016−9026.
(13) Yan, X.; Wang, F.; Zheng, B.; Huang, F. Stimuli-Responsive Supramolecular Polymeric Materials. *Chem. Soc. Rev.* **2012**, *41*, 6042−6065.
(14) Li, S. L.; Xiao, T.; Lin, C.; Wang, L. Advanced Supramolecular Polymers Constructed by Orthogonal Self-Assembly. *Chem. Soc. Rev.* **2012**, *41*, 5950−5968.
(15) Aida, T.; Meijer, E. W.; Stupp, S. I. Functional Supramolecular Polymers. *Science* **2012**, *335*, 813−817.
(16) Dong, R.; Zhou, Y.; Huang, X.; Zhu, X.; Lu, Y.; Shen, J. Functional Supramolecular Polymers for Biomedical Applications. *Adv. Mater.* **2015**, *27*, 498−526.
(17) Smith, K. H.; Tejeda-Montes, E.; Poch, M.; Mata, A. Integrating Top-down and Self-Assembly in the Fabrication of Peptide and Protein-Based Biomedical Materials. *Chem. Soc. Rev.* **2011**, *40*, 4563−4577.
(18) Mulder, A.; Huskens, J.; Reinhoudt, D. N. Multivalency in Supramolecular Chemistry and Nanofabrication. *Org. Biomol. Chem.* **2004**, *2*, 3409−3424.
(19) Hamley, I. W. Self-Assembly of Amphiphilic Peptides. *Soft Matter* **2011**, *7*, 4122−4138.
(20) Iamsaard, S.; Aßhoff, S. J.; Matt, B.; Kudernac, T.; Cornelissen, J. J. L. M.; Fletcher, S. P.; Katsonis, N. Conversion of Light into Macroscopic Helical Motion. *Nat. Chem.* **2014**, *6*, 229−235.
(21) Harada, A.; Takashima, Y.; Nakahata, M. Supramolecular Polymeric Materials via Cyclodextrin-Guest Interactions. *Acc. Chem. Res.* **2014**, *47*, 2128−2140.
(22) van Oosten, C. L.; Bastiaansen, C. W. M.; Broer, D. J. Printed Artificial Cilia from Liquid-Crystal Network Actuators Modularly Driven by Light. *Nat. Mater.* **2009**, *8*, 677−682.
(23) White, T. J.; Broer, D. J. Programmable and Adaptive Mechanics with Liquid Crystal Polymer Networks and Elastomers. *Nat. Mater.* **2015**, *14*, 1087−1098.
(24) Li, Q.; Fuks, G.; Moulin, E.; Maaloum, M.; Rawiso, M.; Kulic, I.; Foy, J. T.; Giuseppone, N. Macroscopic Contraction of a Gel Induced by the Integrated Motion of Light-Driven Molecular Motors. *Nat. Nanotechnol.* **2015**, *10*, 161−165.
(25) Iwaso, K.; Takashima, Y.; Harada, A. Fast Response Dry-Type Artificial Molecular Muscles with [c2]Daisy Chains. *Nat. Chem.* **2016**, *8*, 625−632.
(26) Foy, J. T.; Li, Q.; Goujon, A.; Colard-Itté, J. R.; Fuks, G.; Moulin, E.; Schiffmann, O.; Dattler, D.; Funeriu, D. P.; Giuseppone, N. Dual-Light Control of Nanomachines that Integrate Motor and Modulator Subunits. *Nat. Nanotechnol.* **2017**, *12*, 540−545.
(27) Gelebart, A. H.; Mulder, D. J.; Varga, M.; Konya, A.; Vantomme, G.; Meijer, E. W.; Selinger, R. L. B.; Broer, D. J. Making Waves in a Photoactive Polymer Film. *Nature* **2017**, *546*, 632−636.
(28) Aßhoff, S. J.; Lancia, F.; Iamsaard, S.; Matt, B.; Kudernac, T.; Fletcher, S. P.; Katsonis, N. High-Power Actuation from Molecular Photoswitches in Enantiomerically Paired Soft Springs. *Angew. Chem., Int. Ed.* **2017**, *56*, 3261−3265.
(29) Camacho-Lopez, M.; Finkelmann, H.; Palffy-Muhoray, P.; Shelley, M. Fast Liquid-Crystal Elastomer Swims into the Dark. *Nat. Mater.* **2004**, *3*, 307−310.
(30) Ikeda, T.; Mamiya, J.; Yu, Y. Photomechanics of Liquid-Crystalline Elastomers and Other Polymers. *Angew. Chem., Int. Ed.* **2007**, *46*, 506−528.
(31) Chen, J.; Leung, F. K. C.; Stuart, M. C. A.; Kajitani, T.; Fukushima, T.; van der Giessen, E.; Feringa, B. L. Artificial Muscle-like Function from Hierarchical Supramolecular Assembly of Photoresponsive Molecular Motors. *Nat. Chem.* **2018**, *10*, 132−138.
(32) Leung, F. K. C.; van den Enk, T.; Kajitani, T.; Chen, J.; Stuart, M. C. A.; Kuipers, J.; Fukushima, T.; Feringa, B. L. Supramolecular Packing and Macroscopic Alignment Controls Actuation Speed in Macroscopic Strings of Molecular Motor Amphiphiles. *J. Am. Chem. Soc.* **2018**, *140*, 17724−17733.
(33) Leung, F. K. C.; Kajitani, T.; Stuart, M. C. A.; Fukushima, T.; Feringa, B. L. Dual-Controlled Macroscopic Motions in a Supramolecular Hierarchical Assembly of Motor Amphiphiles. *Angew. Chem., Int. Ed.* **2019**, *58*, 10985−10989.
(34) Ikegami, T.; Kageyama, Y.; Obara, K.; Takeda, S. Dissipative and Autonomous Square-Wave Self-Oscillation of a Macroscopic Hybrid Self-Assembly under Continuous Light Irradiation. *Angew. Chem., Int. Ed.* **2016**, *55*, 8239−8243.

(35) Irie, M.; Fukaminato, T.; Matsuda, K.; Kobatake, S. Photochromism of Diarylethene Molecules and Crystals: Memories, Switches, and Actuators. *Chem. Rev.* **2014**, *114*, 12174−12277.
(36) Kitagawa, D.; Nishi, H.; Kobatake, S. Photoinduced Twisting of a Photochromic Diarylethene Crystal. *Angew. Chem., Int. Ed.* **2013**, *52*, 9320−9322.
(37) Morimoto, M.; Irie, M. A Diarylethene Cocrystal that Converts Light into Mechanical Work. *J. Am. Chem. Soc.* **2010**, *132*, 14172−14178.
(38) Goujon, A.; Mariani, G.; Lang, T.; Moulin, E.; Rawiso, M.; Buhler, E.; Giuseppone, N. Controlled Sol-Gel Transitions by Actuating Molecular Machine Based Supramolecular Polymers. *J. Am. Chem. Soc.* **2017**, *139*, 4923−4928.
(39) Samanta, D.; Gemen, J.; Chu, Z.; Diskin-Posner, Y.; Shimon, L. J. W.; Klajn, R. Reversible Photoswitching of Encapsulated Azobenzenes in Water. *Proc. Natl. Acad. Sci. U. S. A.* **2018**, *115*, 9379−9384.
(40) Grzelczak, M.; Liz-Marzán, L. M.; Klajn, R. Stimuli-Responsive Self-Assembly of Nanoparticles. *Chem. Soc. Rev.* **2019**, *48*, 1342−1361.
(41) van Herpt, J. T.; Areephong, J.; Stuart, M. C. A.; Browne, W. R.; Feringa, B. L. Light-Controlled Formation of Vesicles and Supramolecular Organogels by a Cholesterol-Bearing Amphiphilic Molecular Switch. *Chem. - Eur. J.* **2014**, *20*, 1737−1742.
(42) Wu, A.; Sun, P.; Sun, N.; Zheng, L. Responsive Self-Assembly of Supramolecular Hydrogel Based on Zwitterionic Liquid Asymmetric Gemini Guest. *Chem. - Eur. J.* **2018**, *24*, 10452−10459.
(43) Choi, Y. J.; Kim, J. T.; Yoon, W. J.; Kang, D. G.; Park, M.; Kim, D. Y.; Lee, M. H.; Ahn, S.; Jeong, K. U. Azobenzene Molecular Machine: Light-Induced Wringing Gel Fabricated from Asymmetric Macrogelator. *ACS Macro Lett.* **2018**, *7*, 576−581.
(44) Wang, C.; Chen, Q.; Sun, F.; Zhang, D.; Zhang, G.; Huang, Y.; Zhao, R.; Zhu, D. Multistimuli Responsive Organogels Based on a New Gelator Featuring Tetrathiafulvalene and Azobenzene Groups: Reversible Tuning of the Gel-Sol Transition by Redox Reactions and Light Irradiation. *J. Am. Chem. Soc.* **2010**, *132*, 3092−3096.
(45) Koumura, N.; Kudo, M.; Tamaoki, N. Photocontrolled Gel-to-Sol-to-Gel Phase Transitioning of meta-Substituted Azobenzene Bisurethanes through the Breaking and Reforming of Hydrogen Bonds. *Langmuir* **2004**, *20*, 9897−9900.
(46) Zhou, Y.; Xu, M.; Yi, T.; Xiao, S.; Zhou, Z.; Li, F.; Huang, C. Morphology-Tunable and Photoresponsive Properties in a Self-Assembled Two-Component Gel System. *Langmuir* **2007**, *23*, 202−208.
(47) Kim, J. H.; Seo, M.; Kim, Y. J.; Kim, S. Y. Rapid and Reversible Gel-Sol Transition of Self-Assembled Gels Induced by Photoisomerization of Dendritic Azobenzenes. *Langmuir* **2009**, *25*, 1761−1766.
(48) Zhang, D.; Lu, X.; Li, Y.; Wang, G.; Chen, Y.; Jiang, J. Dual Stimuli-Responsive Wormlike Micelles Base on Cationic Azobenzene Surfactant and Sodium Azophenol. *Colloids Surf., A* **2018**, *543*, 155−162.
(49) Denkov, N. D.; Tcholakova, S.; Golemanov, K.; Ananthpadmanabhan, K. P.; Lips, A. The Role of Surfactant Type and Bubble Surface Mobility in Foam Rheology. *Soft Matter* **2009**, *5*, 3389−3408.
(50) Mileva, E.; Exerowa, D. Amphiphilic Nanostructures in Foam Films. *Curr. Opin. Colloid Interface Sci.* **2008**, *13*, 120−127.
(51) Fameau, A. L.; Salonen, A. Effect of Particles and Aggregated Structures on the Foam Stability and Aging. *C. R. Phys.* **2014**, *15*, 748−760.
(52) Shi, S.; Yin, T.; Shen, W. Switchable Foam Control by a New Surface-Active Ionic Liquid. *RSC Adv.* **2016**, *6*, 93621−93625.
(53) Wan, Z.; Sun, Y.; Ma, L.; Zhou, F.; Guo, J.; Hu, S.; Yang, X. Long-Lived and Thermoresponsive Emulsion Foams Stabilized by Self-Assembled Saponin Nanofibrils and Fibrillar Network. *Langmuir* **2018**, *34*, 3971−3980.
(54) Schnurbus, M.; Stricker, L.; Ravoo, B. J.; Braunschweig, B. Smart Air-Water Interfaces with Arylazopyrazole Surfactants and Their Role in Photoresponsive Aqueous Foam. *Langmuir* **2018**, *34*, 6028−6035.
(55) Chevallier, E.; Monteux, C.; Lequeux, F.; Tribet, C. Photofoams: Remote Control of Foam Destabilization by Exposure to Light Using an Azobenzene Surfactant. *Langmuir* **2012**, *28*, 2308−2312.
(56) Chevallier, E.; Saint-Jalmes, A.; Cantat, I.; Lequeux, F.; Monteux, C. Light Induced Flows Opposing Drainage in Foams and Thin-Films Using Photosurfactants. *Soft Matter* **2013**, *9*, 7054−7060.
(57) Chen, S.; Wang, C.; Yin, Y.; Chen, K. Synthesis of Photo-Responsive Azobenzene Molecules with Different Hydrophobic Chain Length for Controlling Foam Stability. *RSC Adv.* **2016**, *6*, 60138−60144.
(58) Chen, S.; Zhang, Y.; Chen, K.; Yin, Y.; Wang, C. Insight into a Fast-Phototuning Azobenzene Switch for Sustainably Tailoring the Foam Stability. *ACS Appl. Mater. Interfaces* **2017**, *9*, 13778−13784.
(59) Mamane, A.; Chevallier, E.; Olanier, L.; Lequeux, F.; Monteux, C. Optical Control of Surface Forces and Instabilities in Foam Films Using Photosurfactants. *Soft Matter* **2017**, *13*, 1299−1305.
(60) Lei, L.; Xie, D.; Song, B.; Jiang, J.; Pei, X.; Cui, Z. Photoresponsive Foams Generated by a Rigid Surfactant Derived from Dehydroabietic Acid. *Langmuir* **2017**, *33*, 7908−7916.
(61) Jiang, J.; Ma, Y.; Cui, Z. Smart Foams Based on Dual Stimuli-Responsive Surfactant. *Colloids Surf., A* **2017**, *513*, 287−291.
(62) Chen, S.; Fei, L.; Ge, F.; Wang, C. Photoresponsive Aqueous Foams with Controllable Stability from Nonionic Azobenzene Surfactants in Multiple-Component Systems. *Soft Matter* **2019**, *15*, 8313−8319.
(63) Chen, S.; Zhang, W.; Wang, C.; Sun, S. A Recycled Foam Coloring Approach Based on the Reversible Photo-Isomerization of an Azobenzene Cationic Surfactant. *Green Chem.* **2016**, *18*, 3972−3980.
(64) Fameau, A. L.; Saint-Jalmes, A.; Cousin, F.; Houinsou-Houssou, B.; Novales, B.; Navailles, L.; Nallet, F.; Gaillard, C.; Boué, F.; Douliez, J. P. Smart Foams: Switching Reversibly between Ultrastable and Unstable Foams. *Angew. Chem., Int. Ed.* **2011**, *50*, 8264−8269.
(65) Fameau, A. L.; Lam, S.; Velev, O. D. Multi-Stimuli Responsive Foams Combining Particles and Self-Assembling Fatty Acids. *Chem. Sci.* **2013**, *4*, 3874−3881.
(66) Coleman, A. C.; Beierle, J. M.; Stuart, M. C. A.; Maciá, B.; Caroli, G.; Mika, J. T.; van Dijken, D. J.; Chen, J.; Browne, W. R.; Feringa, B. L. Light-Induced Disassembly of Self-Assembled Vesicle-Capped Nanotubes Observed in Real Time. *Nat. Nanotechnol.* **2011**, *6*, 547−552.
(67) Erne, P. M.; van Bezouwen, L. S.; Štacko, P.; van Dijken, D. J.; Chen, J.; Stuart, M. C. A.; Boekema, E. J.; Feringa, B. L. Loading of Vesicles into Soft Amphiphilic Nanotubes Using Osmosis. *Angew. Chem., Int. Ed.* **2015**, *54*, 15122−15127.
(68) van Dijken, D. J.; Chen, J.; Stuart, M. C. A.; Hou, L.; Feringa, B. L. Amphiphilic Molecular Motors for Responsive Aggregation in Water. *J. Am. Chem. Soc.* **2016**, *138*, 660−669.
(69) Israelachvili, J. N.; Mitchell, D. J.; Ninham, B. W. Theory of Self-Assembly of Hydrocarbon Amphiphiles into Micelles and Bilayers. *J. Chem. Soc., Faraday Trans. 2* **1976**, *72*, 1525−1568.
(70) Shimizu, T.; Masuda, M.; Minamikawa, H. Supramolecular Nanotube Architectures Based on Amphiphilic Molecules. *Chem. Rev.* **2005**, *105*, 1401−1443.
(71) Neubauer, T. M.; van Leeuwen, T.; Zhao, D.; Lubbe, A. S.; Kistemaker, J. C. M.; Feringa, B. L. Asymmetric Synthesis of First Generation Molecular Motors. *Org. Lett.* **2014**, *16*, 4220−4223.
(72) Dong, J.; Xun, Z.; Zeng, Y.; Yu, T.; Han, Y.; Chen, J.; Li, Y. Y.; Yang, G.; Li, Y. A Versatile and Robust Vesicle Based on a Photocleavable Surfactant for Two-Photon-Tuned Release. *Chem. - Eur. J.* **2013**, *19*, 7931−7936.
(73) Wang, J.; Feringa, B. L. Dynamic Control of Chiral Space in a Catalytic Asymmetric Reaction Using a Molecular Motor. *Science* **2011**, *331*, 1429−1432.

https://dx.doi.org/10.1021/jacs.0c03153
J. Am. Chem. Soc. 2020, 142, 10163−10172

(74) Lubbe, A. S.; Böhmer, C.; Tosi, F.; Szymanski, W.; Feringa, B. L. Molecular Motors in Aqueous Environment. *J. Org. Chem.* **2018**, *83*, 11008−11018.
(75) Stuart, M. C. A.; van de Pas, J. C.; Engberts, J. B. F. N. The Use of Nile Red to Monitor the Aggregation Behavior in Ternary Surfactant-Water-Organic Solvent Systems. *J. Phys. Org. Chem.* **2005**, *18*, 929−934.
(76) Tantakitti, F.; Boekhoven, J.; Wang, X.; Kazantsev, R. V.; Yu, T.; Li, J.; Zhuang, E.; Zandi, R.; Ortony, J. H.; Newcomb, C. J.; Palmer, L. C.; Shekhawat, G. S.; Olvera de la Cruz, M.; Schatz, G. C.; Stupp, S. I. Energy Landscapes and Functions of Supramolecular Systems. *Nat. Mater.* **2016**, *15*, 469−476.
(77) Yu, H.; Wang, Y.; Zhong, Y.; Mao, Z.; Tan, S. Foam Properties and Application in Dyeing Cotton Fabrics with Reactive Dyes. *Color. Technol.* **2014**, *130*, 266−272.
(78) Karakashev, S. I.; Grozdanova, M. V. Foams and Antifoams. *Adv. Colloid Interface Sci.* **2012**, *176*−*177*, 1−17.
(79) Fameau, A. L.; Houinsou-Houssou, B.; Ventureira, J. L.; Navailles, L.; Nallet, F.; Novales, B.; Douliez, J. P. Self-Assembly, Foaming, and Emulsifying Properties of Sodium Alkyl Carboxylate/Guanidine Hydrochloride Aqueous Mixtures. *Langmuir* **2011**, *27*, 4505−4513.
(80) Fameau, A. L.; Cousin, F.; Derrien, R.; Saint-Jalmes, A. Design of Responsive Foams with an Adjustable Temperature Threshold of Destabilization. *Soft Matter* **2018**, *14*, 2578−2581.
(81) Shin, J. Y.; Abbott, N. L. Using Light to Control Dynamic Surface Tensions of Aqueous Solutions of Water Soluble Surfactants. *Langmuir* **1999**, *15*, 4404−4410.
(82) Cicciarelli, B. A.; Hatton, T. A.; Smith, K. A. Dynamic Surface Tension Behavior in a Photoresponsive Surfactant System. *Langmuir* **2007**, *23*, 4753−4764.
(83) Cicciarelli, B. A.; Elia, J. A.; Hatton, T. A.; Smith, K. A. Temperature Dependence of Aggregation and Dynamic Surface Tension in a Photoresponsive Surfactant System. *Langmuir* **2007**, *23*, 8323−8330.
(84) Chevallier, E.; Mamane, A.; Stone, H. A.; Tribet, C.; Lequeux, F.; Monteux, C. Pumping-out Photo-Surfactants from an Air-Water Interface Using Light. *Soft Matter* **2011**, *7*, 7866−7874.
(85) Cohen, A.; Fraysse, N.; Raufaste, C. Drop Coalescence and Liquid Flow in a Single Plateau Border. *Phys. Rev. E* **2015**, *91*, 1−12.

https://dx.doi.org/10.1021/jacs.0c03153
J. Am. Chem. Soc. 2020, 142, 10163−10172